A template of rat brain based on fMRI T_2^* imaging*

HU Zhenghui[1], WU Yigen[2], WANG Xiaochuan[3], WANG Jianzhi[3], CHEN Feiyan[1] and TANG Xiaowei[1]**

(1. Department of Physics and Bio-X Laboratory, Zhejiang University, Hangzhou 310027, China; 2. Institute of High Energy Physics and Key Laboratory of Nuclear Analysis Techniques, Chinese Academy of Sciences, Beijing 100039, China; 3. Department of Pathophysiology, Tongji Medical College, Huazhong University of Science and Technology, Wuhan 430030, China)

Received October 9, 2004; revised November 11, 2004

Abstract The development of functional magnetic resonance imaging (fMRI) technology has made it possible to carry out functional brain imaging experiments in small animals. Usually, group data is required to form the assessment of population, which can not only increase the sensitivity of the overall experiment, but also allow the generalization of the conclusion to the whole population. In order to average the signals of functional brain images from different subjects, it is necessary to put all the mapping images into the same standard space (template image). However, up to now, most animal brain templates remain unavailable and it must be done by ourselves. In this study, a template image based on the brains of eight male Wistar rats is obtained and it is successfully used in our present Alzheimer disease (AD)-like rat model studies as template for spatially normalizing images to the same stereotaxical space. The fMRI results processed with statistical parametric mapping (SPM99) software are in agreement with the results from immunohistochemical experiment, which proves that this method is universally applicable to the pathologic models of other small animals and to human brain lesion studies.

Keywords: fMRI, animal model, atlas, template, normalization, T_2^*.

The development of noninvasive functional neuroimaging methods has made it possible to investigate large-scale activation patterns of brain. FMRI, a representative in hemodynamic techniques, has been used extensively in the studies of the physiology, pathology and psychology of brains[1—3], for its less invasive property, superior resolution, and lower cost compared to PET techniques.

It is important to point out that common image analysis softwares such as statistical parametric mapping (SPM), analyses of functional neuroimages (AFNI), create data by doing a separately statistical analysis voxel by voxel. Obviously, in order to implement voxel-based analysis of imaging data, the data from different subjects must be derived from homologous parts of the brain. In imaging neuroscience, it has been named the operation of spatial normalization, which facilitates inter-subject averaging of data as well, and allows the generalization of any conclusion to the whole population. This means that it is necessary to average signals over a number of subjects in order to obtain a meaningful result in most cases. In addition, another advantage of spatially normalized images is that activations can be readily incorporated into ongoing brain atlas and database projects, such as one developed by the International Consortium for Human Brain Mapping (ICBM), thus meaningful coordinates can be given for the centers of activation. Usually, the atlas of Talairach and Tournoux is used for human studies[4]. However, the analogous common space is unavailable for animal studies.

Brain atlases are graphical representations of neuroanatomy, which are of fundamental importance to the whole of neuroscience. They provide a means of navigating through neural tissue for experiments and a standardized coordinate system for reporting spatially distributed neuronal properties. However, when only a standard coordinate system is required to specify the location, a template is sufficient. The simplest way to solve this problem is to get the mean image of a single subject from the group being studied. Then, it can be used as the template for normalization of all subjects.

The purpose of this study is to create a representative template of rat brain based on SPM from a co-registered group of subjects positioned stereotaxically and to produce better normalizations for our study of

* Supported by the Major State Basic Research Development Program of China (Grant No. 19990504000)

** To whom correspondence should be addressed. E-mail: tangxw@zju.edu.cn

pathological model of rats[5].

1 Materials and methods

Eight male Wistar rats (2 months old, body weight 250 ± 25 g, Grade II Certificate No. TJLA2000-3) were from Faculty of Laboratory Animal (Tongji Medical College of HUST, China), and maintained according to the Chinese Regulations for Experimental Animals for 9 days. The rats were anesthetized with intraperitoneal injections of 60 g/L chloral hydrate. The AD-like rat model was developed by injection of 2 μL of 10 mmol/L isoproterenol (IP) into ventral dura (DV) 3 mm in depth as described previously[5]. The same volume of normal saline (NS) was injected as vehicle control. Every rat was placed prone in a cradle in turn and its head was secured with a bite-bar and tightly fixed by foam cushions on both sides of the head to minimize head movement.

All MRI data were obtained on a horizontal-bore 4.7T spectrometer (Bruker Biospec 47/30) in Wuhan Institute of Physics and Mathematics, Chinese Academy of Sciences. The center of the special radio-frequency surface coil (10 mm in diameter) was placed above the bregma and static magnetic field homogeneity was optimized on axial slices. A gradient echo fast imaging sequence (GEFI, T_2^*-weighted) with a small shot angle was selected to maximize the blood oxygen level-dependent contrast (echo time 25 ms, repeat time 560 ms, flip angle 40°). Interleave samplings were applied to avoid interference. Each brain image volume was acquired from 14 slices, each 1 mm thick with 0.2 mm gaps between adjacent layers and comprising 256×256 pixels for each slice. Each scanning session consists of about 35 image volumes. Acquisition time of each image volume was 1 min and 11 seconds. All data were acquired under steady-state conditions without inflicting any stimulus.

After completion of fMRI, immunohistochemistry assay was carried out for the brain tissues as described previously[5].

2 Data analysis and processing

The first four scans were removed to eliminate saturation effects and the remainder then was used for analysis. SPM99 (Wellcome Department of Cognitive Neurology, London, http://www.fil.ion.ucl.ac.uk/spm) was used for our fMRI data preprocessing and statistical analysis.

An example of a high resolution axial image acquired with the final pulse sequence is shown in Fig. 1, where the pixel size was magnified to fourfold of the original ones (0.234 mm×0.234 mm×1.2 mm) to make the rat brain a similar scale to human brain for satisfying requirements of SPM. A mass of non-brain structure can be observed on the left of the figure, and an image after brain extraction is shown on the right, where the signal out of the brain was preset to zero. For most cases, we are interested in the brain, not the surrounding tissues such as scalp, skull or eyeballs. Since these non-brain structures vary significantly between individuals or between scans of the same individual, it is necessary to remove these structures before structural analysis. As shown in Fig. 1, the brain tissue was distinguished using our software from other tissues. It is worth noticing that, for the purpose of registration, small errors at this stage have little effect on registration result.

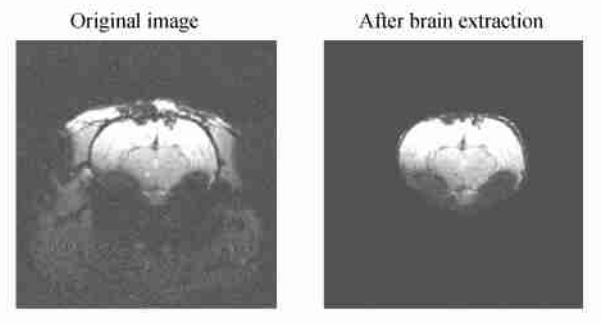

Fig. 1. An illustration of manually removed non-brain structures using our software.

During a series of scans, a subject will move inevitably. Since fMRI is very sensitive to the motion, it is necessary to have an accurate motion correction before averaging. Also, it can increase the sensitivity of the experiment. When SPM analysis by t-test is based on the signal change relative to the residual variance, and movement artifacts will enhance this residual variance, the sensitivity of the test to true activations is reduced. The purpose of motion correction is to determine some optimal parameters for decreasing the residual variance between the linear model and real observation data.

It is a prevalent way that other scans of a session are realigned to the first image in the selected series[6]. For realignment of an image time-series of the same modality, it is reasonable that movement correction is considered as rigid body transformations. In three dimensions a rigid body transformation can be defined by six parameters. These parameters are, typically, three translations and three rotations about orthogonal axes, respectively. A matrix, which is used to implement the translation, can be defined as:

$$\boldsymbol{T}=\begin{pmatrix}1&0&0&x_0\\0&1&0&y_0\\0&0&1&z_0\\0&0&0&1\end{pmatrix}, \tag{1}$$

and the matrixes, which are used to carry out rotation (θ, φ and ψ) on the x, y and z axes respectively, expressed as:

$$\boldsymbol{R}_x=\begin{pmatrix}1&0&0&0\\0&\cos(\theta)&\sin(\theta)&0\\0&-\sin(\theta)&\cos(\theta)&0\\0&0&0&1\end{pmatrix},$$

$$\boldsymbol{R}_y=\begin{pmatrix}\cos(\varphi)&0&\sin(\varphi)&0\\0&1&0&0\\-\sin(\varphi)&0&\cos(\varphi)&0\\0&0&0&1\end{pmatrix},$$

$$\boldsymbol{R}_z=\begin{pmatrix}\cos(\psi)&\sin(\psi)&0&0\\-\sin(\psi)&\cos(\psi)&0&0\\0&0&1&0\\0&0&0&1\end{pmatrix}.$$

For each point (x, y, z) in an image, an affine mapping that transforms (x, y, z) into the coordinate of another space (x', y', z') can be expressed in the form of

$$\begin{pmatrix}x'\\y'\\z'\\1\end{pmatrix}=\boldsymbol{T}\circ\boldsymbol{R}_x\circ\boldsymbol{R}_y\circ\boldsymbol{R}_z\circ\begin{pmatrix}x\\y\\z\\1\end{pmatrix}. \tag{2}$$

These estimates are then used to realign the images and to perform a mathematical adjustment to remove movement-related component that persists after simple realignment. The adjustment procedure is based on a moving average-auto-regression model of spin-excitation history effects. The latter components can be prominent and are specific to the way the fMRI signal is acquired.

We assume that the difference between the voxel intensities of reference (the selected first image) and object images can be expressed as

$$ug(x)=f(Mx)+\varepsilon(x), \tag{3}$$

where u is a simple scaling, M is a set of parameters that define the transformation and $\varepsilon(x)$ is some error scalar function. Then, the optimal solution of Eq. (3) can be determined by iteratively solving (for u and M)

$$(A)(u, m_{11}, m_{21}, m_{31}, m_{12}, m_{22}, \cdots, m_{34})^{\mathrm{T}}=f, \tag{4}$$

where f is the object image (treated as a column vector) and matrix $\boldsymbol{A}$ consists of

$$\begin{pmatrix}g&\frac{\partial f}{\partial m_{11}}&\frac{\partial f}{\partial m_{21}}&\frac{\partial f}{\partial m_{31}}&\frac{\partial f}{\partial m_{12}}&\frac{\partial f}{\partial m_{22}}&\cdots&\frac{\partial f}{\partial m_{34}}\end{pmatrix}.$$

Here g is the reference image (the selected first image) and $\partial f/\partial m\cdots$ are column vectors containing the derivative of image f with respect to each parameter. A full exposition of affine transformation algorithm can be found in Ref. [7].

In all image volumes, we discarded the images with head motion greater than one pixel. Each of the rest volumes was re-realigned to the first volume for further analysis. This is reasonable for that (i) these fMRI images are based on resting instead of task-related dynamic changes in oxygen-dependent signal[8], therefore they are not time series; (ii) the effect caused by earlier scans on subsequent scans (due to differential spin-excitation histories mainly) can be ignored because of a longer TR time.

The mean estimated head motion for all eight subjects was minimal and is summarized in Tables 1 and 2. The numbers in the table represent the fraction of pixel length translationally or rotationally moved during whole scans. For example, $\mu_x=0.1$ means that head motion was less than 0.023 mm in the x direction (10% of pixel size 0.234 mm). As shown in Tables 1 and 2, no significant statistical difference was found between these scans.

Table 1. Averaged data of head translation motion for all eight subjects

Subject	Translations					
	Mean			SD[a]		
	μ_x	μ_y	μ_z	σ_x	σ_y	σ_z
1	−0.01	−0.03	−0.02	0.02	0.02	0.01
2	0.04	0.10	0.07	0.02	0.05	0.03
3	0.10	0.05	0.03	0.06	0.12	0.04
4	−0.08	−0.15	0.05	0.09	0.05	0.02
5	0.07	0.02	−0.07	0.06	0.06	0.02
6	0.05	−0.23	0.01	0.07	0.08	0.04
7	0.07	−0.03	−0.07	0.06	0.04	0.02
8	−0.01	0.11	−0.02	0.07	0.07	0.07

[a] Square root of standard deviation for a single pixel.

Table 2. Averaged data of head rotation motion for all eight subjects

Subject	Rotations					
	Mean			SD[a]		
	μ_Φ	μ_Ψ	μ_Ω	σ_Φ	σ_Ψ	σ_Ω
1	−7.01E-04	−1.91E-04	3.03E-04	0.0006	0.0004	0.0005
2	2.38E-03	−4.29E-04	1.32E-03	0.0012	0.0004	0.0007
3	9.62E-04	4.27E-04	1.18E-03	0.0022	0.0003	0.0014
4	3.48E-03	2.40E-03	1.99E-03	0.0014	0.0017	0.0014
5	4.63E-04	1.28E-03	−1.58E-04	0.0007	0.0007	0.0020
6	−3.54E-03	−4.68E-03	6.31E-03	0.0014	0.0017	0.0022
7	−8.98E-04	5.36E-04	−3.12E-03	0.0007	0.0010	0.0022
8	2.34E-03	−7.80E-07	1.60E-03	0.0020	0.0019	0.0021

[a] Square root of standard deviation for a single pixel.

After the realignment process, we got the mean image of all the functional MRI images for each subject. Next, we should coregister all subject to a target image. However, for co-registration between subjects there is an affine transformation rather than a rigid body. Therefore, we selected a subject mean image as an initial target for inter-subject registration, other images were registered to this target with mutual information[9, 10], which is based on measuring the joint entropy of the intensities. For two images A and B, mutual information I can be defined as

$$I(A, B) = H(A) + H(B) - H(A, B),$$

where $H(A)$, $H(B)$ are Shannon entropy of single images A and B, respectively. $H(A, B)$ is the joint entropy for A and B. The marginal (individual) entropies $H(A)$ and $H(B)$ are given by

$$H(A) = -\sum_i p(A_i)\log p(A_i),$$

where $p(A_i)$, $p(B_i)$ are probabilities of grey value in corresponding images.

The Shannon entropy for a joint distribution is defined similarly, only using the joint histogram rather than the individual image histograms,

$$H(A, B) = -\sum_{i,j} p(A_i, B_j)\log p(A_i, B_j),$$

where $p(A_i, B_j)$ is a probability of the grey values in feature space. The feature space is formed by assigning a bin number to each voxel in both images based on the intensity at that voxel. Then a two-dimensional array of bins is formed with the bin numbers for the first image along the vertical axis and those for the second image along the horizontal axis. This array is the joint histogram and to fill it requires looking at each voxel position in turn, finding the bin numbers from each image at this position, then adding one to the cell corresponding to the pair of bin numbers found. Registration is assumed to correspond to maximizing mutual information: the images have to be aligned in such a manner that the amount of information they contain about each other is maximal.

Finally all the coregistered images were subject to average arithmetic to create a mean template image. Before using the template to do normalization, the image will be smooth by 2 times of the pixel width (Fig. 2).

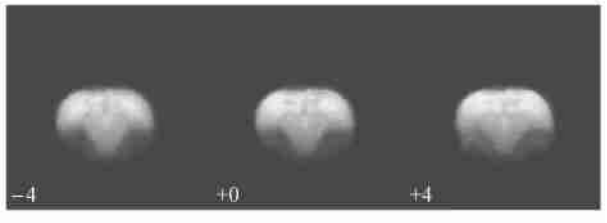

Fig. 2. Three slices from final template images based on all eight rats. The maps from left to right are up to down of the brain, with interval 4.8mm. The displayed brain images are magnified to four-fold of the original ones.

3 Results and discussion

Using our brain template the image processing was performed, and the preprocessed data were analyzed by statistical parametric mapping. A student t-test was applied to find out the difference in signal intensity between AD-like rats and NS-treated rats ($t > 30$, uncorrected, Fig. 3). However, this template is still probably inaccurate. To address this problem, immunohistochemical staining with phosphorylation dependent tau antibodies, which includes tau-1 (recognize unphosphorylated tau at Ser199/Ser202), PHF-1 (recognize phosphorylated tau at Ser396/Ser404) and 12E8 (recognize phosphorylated tau at Ser262/Ser356), was performed. These rats were selected at random from the MRI scanned group (8 IP-treated and 8 NS-treated rats). Much stronger signals of 12E8 and PHF-1 were found in CA1, CA2, CA3, CA4, dentate gyrus regions and the cerebral cortex of IP-treat rats than those in NS-treated ones, which indicates that tau was hyperphosphorylated at

12E8 sites and PHF-1 sites (Fig. 3). The staining of tau-1 in CA1, CA2, CA3, CA4, dentate gyrus regions of IP-treated rats was weaker than that of control ones. However, no obvious difference was observed between the two groups in the cerebral cortex region (Fig. 3), which indicates that tau is hyperphosphorylated at Ser-198/Ser-199/Ser-202 sites in hippocampus, but not in the cortex region. Detailed histological observation was obtained in the earlier study[5]. A negative correlation was found between tau hyperphosphorylation and blood oxygenation level dependent (BOLD) signal intensity in hippocampus and cortex area of IP-treats rats[11]. Namely, with a weakened BOLD signal in the CA1, CA2, CA3, CA4 region and dentate gyrus, tau was found to become hyperphosphorylated at 12E8 epitopes in the same regions. A similar negative correlation was also observed in different regions of cortex using the present new method (Fig. 3), which demonstrates to a certain extent that the template is effective.

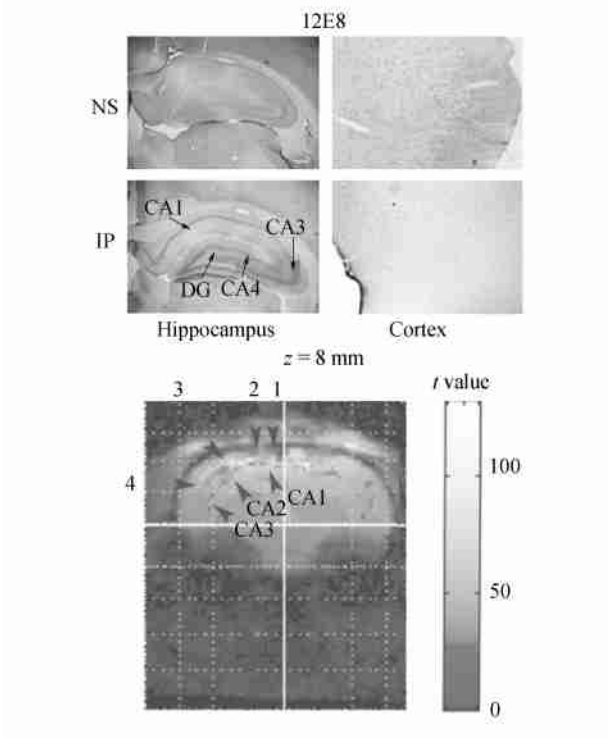

Fig. 3. Comparison of histochemical staining for 12E8 antibody with BOLD observed with fMRI. The frontal lobe cortex area II (1), frontal lobe cortex area I (2), cortical hind limb area (3) and parietal lobe cortex area I (4), are identified[5].

Although a template is sufficient for comparing the locations of activations or lesions between the two groups, it cannot provide enough information on tissue structure. Further studies should focus on establishing a rat brain atlas containing any kinds of information, such as histological or anatomical data. The rat brain template established in this study can be expanded to other animal brain fMRI studies, brain lesion studies and neurodegenerative disorders such as Parkinson's disease in future.

Acknowledgments The authors would like to thank Drs. Feng Yu, Yang Yunhuang for performing the fMRI experiment, to Professors Li Liyun and Liu Maili for their helpful discussions. Specially, we thank the following people for their enthusiastic help and thoughtful suggestions: Prof. Toby Roberts (The Maudsley Advancing Mental Health Care, King's College London), Prof. Du Yiping (Department of Psychiatry and Radiology, University of Colorado Health Science Center), and Prof. Cheng Kang (Japan Science and Technology Corporation).

References

1 Harrington D. L. and Haaland K. Y. Neural underpinning of temporal processing: a review of focal lesion, pharmacological, and functional imaging research. Neuroscience, 1999, 10: 91—116.
2 Cabeza R. and Nyberg L. Imaging cognition II: an empirical review of the 275 PET and fMRI studies. Journal of Cognitive Neuroscience, 2000, 12: 1—47.
3 Li S. J., Biswal B., Li Z. et al. Cocaine administration decreases functional connectivity in human primary visual and motor cortex as detected by functional MRI. Magnetic Resonance in Medicine, 2000, 43: 45—51.
4 Talairach J. and Tournoux P. Co-Planar Stereotaxic Atlas of the Human Brain. New York: Thieme Medical, 1988.
5 Wang X. C., Hu Z. H., Fang Z. Y. et al. Correlation of Alzheimer-like tau abnormal hyperphosphorylation and fMRI BOLD signal intensity. Current Alzheimer Research, 2004, 1(2): 143—145.
6 Friston K. J., Williams S. C. R., Howard R. et al. Movement-related effects in fMRI time series. Magnetic Resonance in Medicine, 1996, 35: 346—355.
7 Woods R. P., Cherry S. R. and Mazziotta J. C. A rapid automated algorithm for accurately aligning and reslicing positron emission tomography images. Journal of Computer Assisted Tomography, 1992, 16: 620—633.
8 Small S. A., Wu E. X., Bartsch D. et al. Imaging physiologic dysfunction neurotechnique of individual hippocampal subregions in humans and genetically modified mice. Neuron, 2000, 28: 653—664.
9 Collignon A., Maes F., Delaere D. et al. Automated multi-modality image registration based on information theory. In: Information Processing in Medical Imaging. Dordrecht: Kluwer Academic Publishers, 1995, 263—274.
10 Viola P. and Wells W. M. III. Alignment by maximization of mutual information. In: International Conference on Computer Vision. Los Alamitos: IEEE Computer Society Press, 1995, 16—23.
11 Hu Z. H., Wang X. C., Li L. Y. et al. Correlation of behavior changes and fMRI BOLD signal in an Alzheimer-like rat model. Acta Biochimica et Biophysica Sinica, 2004, 12: 803—810.